32nd URSI GASS, Montreal, 19–26 August 2017

Proposal of Inverse Doherty Rectifier Tolerant of DC Load Fluctuation

Naoki Sakai(1), Yoichiro Miyazaki(1), Shinji Abe(1), and Takashi Ohira(1)
(1) Department of Electrical and Electronics Information Engineering Toyohashi University of Technology, Toyohashi, Aichi 441-8580 Japan

Abstract

This paper presents a novel RF rectifier that compresses RF input impedance fluctuation caused by DC load change for reducing return loss at RF input power. The proposed rectifier connects twin basic RF rectifiers and a quarter-wave impedance transformer. The proposed rectifier automatically switches the two rectifiers according to DC load resistance. As the result, the rectifier can keep low deviation of RF input impedance. This paper formulates the RF input impedance behavior and verifies its formula by circuit simulation.

1 Introduction

Wireless power transfer system can be applied to a variety of electronic systems such as an electric vehicles, televisions, PCs and mobile phones[1, 2]. The system is required to feed RF power at high efficiency into the load. Because most applications generally require DC power supplies, the system has to employ RF rectifiers to supply DC power. The system engineers are expected to design RF rectifiers having high RF-to-DC conversion efficiency.

To obtain high conversion efficiency, the engineers reduce a return loss at input port of the RF rectifier by an impedance matching circuit. However, it is difficult to reduce return loss of the RF rectifier for the WPT system. Because, the RF input impedance is directly proportional to DC load[3]. Electronic devices frequently changes DC load. Thus, reflection loss is caused by fluctuation of the DC load even though the rectifier emploies impedance matching.

To solve this problem, a scheme which combines a DC/DC converter and an RF rectifier was proposed[4]. Because the DC/DC converter of this scheme can suppress the fluctuation of DC load, the RF input impedance becomes a constant. Therefore, engineers can design the impedance matching circuit for getting high conversion efficiency. However, overall conversion efficiency suffers from the power loss in the DC/DC converter.

This paper presents a novel RF rectifier topology that compresses RF input impedance fluctuation caused by DC load change.

2 Circuit topology

We show the proposed rectifier topology in Fig.1, and describe about principle of behavior. In the proposed rectifier, one basic RF rectifier #A and the same basic RF rectifier #B with a quarter-wave impedance transformer are parallel connected. The basic RF rectifier means topologies such as single-shunt, single-series, bridge, double current, and double voltage. The RF input impedance of the basic RF rectifier is directly proportional with a DC load[3]. On the other hand, in the basic rectifier with the impedance transformer, the RF input impedance is inversely proportional with a DC load. Thus, RF input current i_{in} flows to RF rectifier #A on low DC load, or flows to RF rectifier #B on high DC load. Namely, the proposed rectifier automatically switches into the basic rectifier which has lower RF input impedance. As the result, the proposed rectifier keeps low RF input impedance and compresses RF input impedance fluctuation caused by DC load fluctuation. For the reason that these operation and topology of the proposed rectifier is greatly similar to Doherty amplifier, we name the proposed rectifier topology "Inverse Doherty Rectifier".

3 Impedance Formulation

We derive RF input impedance Z_{in} of the inverse Doherty rectifier. From the RF input impedance is directly proportional to DC load in the basic rectifier, RF input impedance

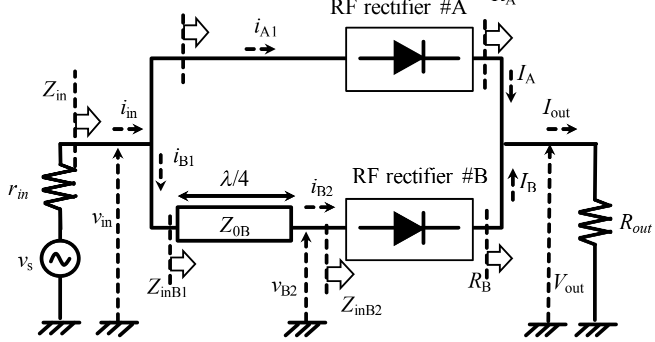

Figure 1. Proposed topology of Inverse Doherty rectifier.

of RF rectifier #A is

$$Z_{inA1} = \frac{R_A}{\rho}, \tag{1}$$

where ρ is proportionality constant which depends on topology of basic rectifier. From Eq.(1) , input impedance Z_{inB1} of RF rectifier #B with the quarter-wave impedance transformer becomes

$$\begin{aligned} Z_{inB2} &= \frac{R_B}{\rho}, \\ Z_{inB1} &= \frac{Z_{0B}^2}{Z_{inB2}} = \frac{Z_{0B}^2 \rho}{R_B}, \end{aligned} \tag{2}$$

which is inversely proportional to DC load R_B. Because RF rectifier #A is connected in parallel to RF rectifier #B, input impedance Z_{in} of inverse Doherty rectifier obtain

$$\begin{aligned} Z_{in} &= \frac{1}{\dfrac{1}{Z_{inA1}} + \dfrac{1}{Z_{inB1}}} \\ &= \frac{Z_{0B}^2 R_A \rho}{Z_{0B}^2 \rho^2 + R_A R_B}. \end{aligned} \tag{3}$$

Next, we derive relation to DC load R_{out} with R_A and R_B in Eq.(3). The DC output load simply represents resistance R since output DC voltage V and DC current I. And output DC current I_A, I_B, and I_{out} satisfy Kirchhoff's law. R_a and R_b are therefore written as

$$R_A = \frac{V_{out}}{I_A},\ R_B = \frac{V_{out}}{I_B},\ R_{out} = \frac{V_{out}}{I_{out}}.$$

$$\alpha = \frac{I_B}{I_A}, \tag{4}$$

$$I_{out} = I_A + I_B,\ I_A = \frac{I_{out}}{\alpha+1},\ I_B = \frac{\alpha I_{out}}{\alpha+1}$$

$$R_A = R_{out}(\alpha+1),\ R_B = \frac{R_{out}}{\alpha}(\alpha+1), \tag{5}$$

where α stands for ratio of current I_A to I_B. For I_A and I_B are non-negative real numbers, α is positive real numbers. Thus Z_{in} substituting Eq.(5) into Eq.(3) obtains

$$Z_{in} = \frac{Z_{0B}^2 R_{out}(\alpha+1)\rho}{Z_{0B}^2 \rho^2 + R_{out}^2 \dfrac{(\alpha+1)^2}{\alpha}}. \tag{6}$$

Last, replace α which is unknown parameter with DC load R_{out}. In the basic rectifier, consider relation to RF input power with DC output power,

$$\eta P_{inA} = P_{outA}, \tag{7}$$

where η is constant depending on the topologies. In other words, η is conversion efficiency including only insertion loss. For relation between power and current

$$P_{inA} = \frac{1}{2}|i_{A1}|^2 Z_{inA1},\ P_{outA} = I_A^2 R_A, \tag{8}$$

Eq.(7) can be transformed into relation to RF input current with DC output current

$$I_A = \sqrt{\frac{\eta}{2\rho}}|i_{A1}|,\ I_B = \sqrt{\frac{\eta}{2\rho}}|i_{B2}|. \tag{9}$$

The input current i_{B2} flowing out quarter-wave impedance transformer is represented by input voltage v_{in}

$$i_{B2} = -j\frac{v_{in}}{Z_{0B}}. \tag{10}$$

Therefore, α of Eq.(4) replaced by current of Eq.(9) and Eq.(10) is shown in

$$\alpha = \frac{\sqrt{\dfrac{\eta}{2\rho}}\left|-j\dfrac{v_{in}}{Z_{0B}}\right|}{\sqrt{\dfrac{\eta}{2\rho}}|i_{A1}|} = \frac{|Z_{inA1}|}{Z_{0B}}. \tag{11}$$

In addition, substituting Eq.(5) and Eq.(1) for the above equation, we get

$$\begin{aligned} \alpha &= \frac{R_{out}(\alpha+1)}{Z_{0B}\rho} \\ \alpha &= \frac{1}{\dfrac{Z_{0B}\rho}{R_{out}} - 1}. \end{aligned} \tag{12}$$

From the condition that α is positive real number, range of DC load R_{out} in the above equation is $0 < R_{out} \le Z_0\rho$. Thus, on DC load R_{out} fluctuation, we reach the Z_{in} characteristic

$$\begin{aligned} Z_{in} &= \frac{Z_{0B}^2 R_{out}\alpha\rho}{Z_{0B}^2\rho^2 \dfrac{\alpha}{\alpha+1} + R_{out}^2(\alpha+1)} \\ &= \frac{Z_{0B}^2 R_{out}\rho \dfrac{R_{out}}{Z_{0B}-R_{out}}}{Z_{0B}^2\rho^2 \dfrac{R_{out}}{Z_{0B}\rho} + R_{out}^2 \dfrac{Z_{0B}\rho}{Z_{0B}\rho - R_{out}}} \\ &= \frac{R_{out}}{\rho}. \end{aligned} \tag{13}$$

When DC load R_{out} gets $Z_{0B}\rho$, DC output current I_{A1} gets zero due to $\alpha = \infty$ and $I_{A1}, I_{B1} \ge 0$. Similarly, when R_{out} become higher than $Z_{0B}\rho$, we assume that I_{A1} gets zero. Namely the basic rectifier #A doesn't drive on above range. Thus Z_{in} obtains the same

$$Z_{in} = \frac{Z_{0B}^2\rho}{R_{out}} \tag{14}$$

as Eq.(2). By concluding above equations, input impedance Z_{in} of inverse Doherty rectifier behaves as

$$Z_{in} = \begin{cases} \dfrac{R_{out}}{\rho} & (0 < R_{out} \le Z_{0B}\rho) \\ \dfrac{Z_{0B}^2\rho}{R_{out}} & (R_{out} > Z_{0B}\rho) \end{cases} \tag{15}$$

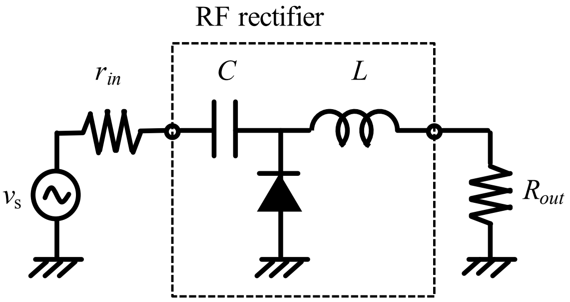

Figure 2. Conventional rectifier schematic as a reference.

If the DC load R_{out} fluctuates as an example, let us show input impedance Z_{in} and reflection coefficient $|\Gamma|$ characteristic of the inverse Doherty rectifier which employs single-shunt rectifier as the basic rectifier. The single-shunt rectifier topology is shown Fig.2 and Z_{0B} equals 70Ω. From Eq.(1) and Eq.(15), the Z_{in} and $|\Gamma|$ characteristics of the single-shunt rectifier and the inverse Doherty rectifier are represented in Fig.3, Fig.4. In the single-shunt rectifier, range of R_{out} in which $|\Gamma|$ becomes below 1/6 is from 30Ω to 70Ω. And, in the inverse Doherty rectifier, the range of R_{out} is from 30Ω to 163Ω which is about 3 times as large as the single-shunt. The inverse Doherty rectifier is able to keep low reflection coefficient, in other words, it has reached to compress fluctuation of RF input impedance caused by DC load change.

4 Circuit simulation

We investigate behavior of the inverse Doherty rectifier as shown in Fig. 5, and validity of Eq.(15) by a circuit simulation. The inverse Doherty rectifier employs ideal diodes and ideal quarter-wave impedance transformer in the simulation. In the rectifier, inductance L is 500μH, capacitance C is 50nH, and transmission line characteristic impedance Z_{0B} is 70Ω. An RF power supply outputs 1 W at 10 MHz. The circuit simulator we employ is Keysight Advanced Design System.

Figure 6 shows current flows i_{A1}, i_{B1} and i_{in} changed by DC load. This result shows that the rectifier #B is mainly driven under the low DC load, the rectifier #A is driven under the high DC load. Dependence of Z_{in} and $|\Gamma|$ on the DC load R show Fig. 7 and 8. The simulated results of Fig. 7 and 8 extremely correspond with the formulated results of Fig. 3 and 4. Therefore, Eq.(15) is correct formula.

5 Conclusion

This paper represented a novel RF rectifier topology named "inverse Doherty rectifier", and formulated its RF input impedance behavior. The RF input impedance formula expresses that inverse Doherty rectifier can compress RF input impedance fluctuation caused by DC load change. Simulated behavior of the RF input impedance extremely corresponds with the formulated behavior. Therefore, the inverse Doherty rectifier will contribute to future wireless power transfer systems.

Acknowledgment

This work was supported in part by the government of Japan (contract: MIC SCOPE Program #0159-0001), and

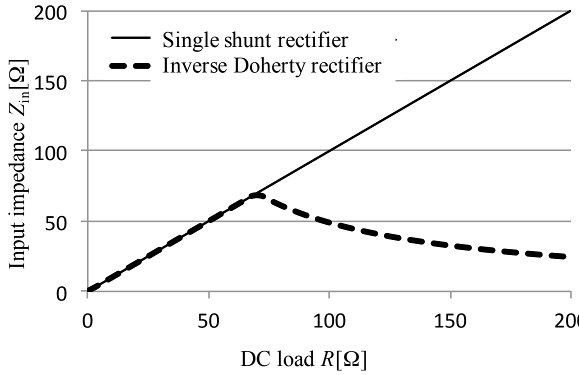

Figure 3. Tolerance improvement to DC load fluctuation (formulated).

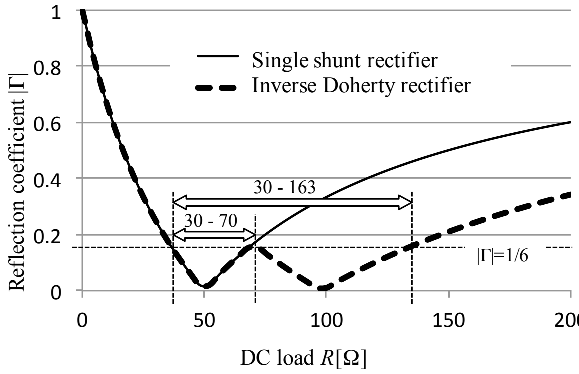

Figure 4. Acceptable DC load range extension to meet $|\Gamma| \leq 1/6$ (formulated).

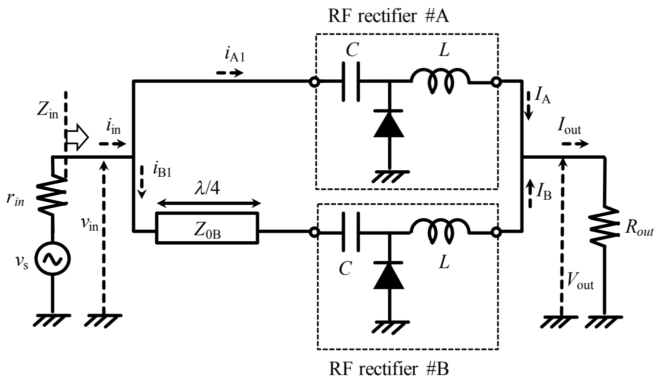

Figure 5. Detailed circuit schematic for simulation.

VLSI Design and Education Center(VDEC), the University of Tokyo in collaboration with Keysight Technologies Japan, Ltd.

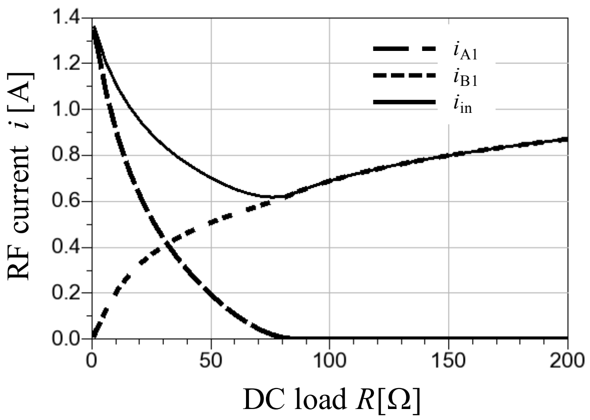

Figure 6. Input current distribution changed by DC load. (simulated)

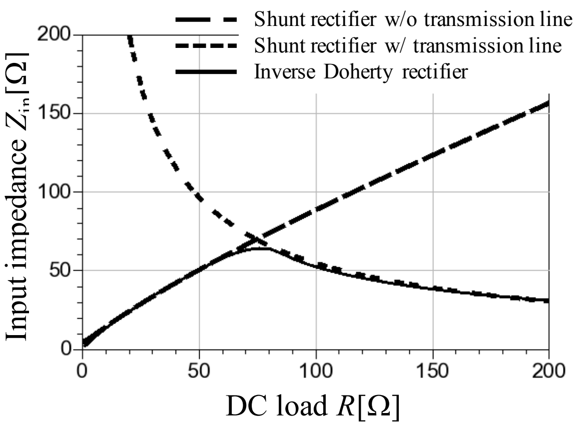

Figure 7. Tolerance improvement to DC load fluctuation (simulated).

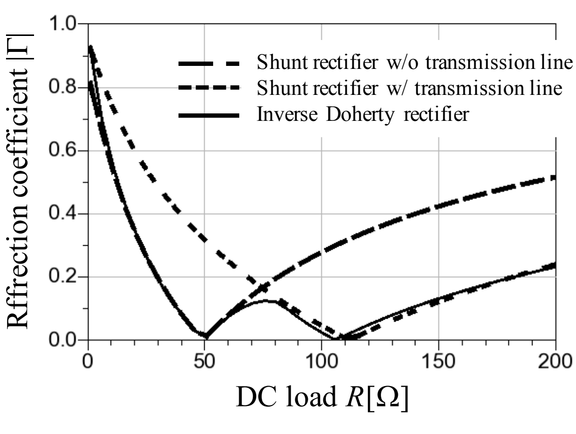

Figure 8. Acceptable DC load range extension to meet $|\Gamma| \leq 1/6$ (simulated).

References

[1] N. Shinohara, "Power without wires," *IEEE Microwave Magazine*, vol.12, no.7, pp.S64-S73, Dec. 2011.

[2] S. Choi, J. Huh, W.Y. Lee, S.W. Lee, and C.T. Rim, "New cross-segmented power supply rails for roadway-powered electric vehicles," *IEEE Trans. Power Electronics*, vol.28, no.12, pp.5832-5841, Dec. 2013.

[3] T. Ohira, "Power efficiency and optimum load formulas on RF rectifiers featuring flow-angle equations," *IEICE Electronics Express*, vol.10, no.11, pp.1-9, June 2013.

[4] G. Lovison, M. Sato, T. Imura, and Y. Hori, "Secondary-side-only simultaneous power and efficiency control for two converters in wireless power transfer system," in *Proc. IEEE Ind. Electron. Soc. Conf.*, pp. 4824-4829, Yokohama, Nov. 2015.